Published in final edited form as:
Clin Cancer Res. 2010 October 1; 16(19): 4742–4754. doi:10.1158/1078-0432.CCR-10-0529.

Role of C/EBP homologous protein (CHOP) in Panobinostat-mediated potentiation of Bortezomib-induced lethal ER stress in Mantle Cell Lymphoma cells

Rekha Rao[1], **Srilatha Nalluri**[1], **Warren Fiskus**[1], **Andrew Savoie**[1], **Kathleen M Buckley**[1], **Kyungsoo Ha**[1], **Ramesh Balusu**[1], **Atul Joshi**[1], **Veena Coothankandaswamy**[1], **Jianguo Tao**[2], **Eduardo Sotomayor**[2], **Peter Atadja**[3], and **Kapil N. Bhalla**[1]

[1] Medical College of Georgia Cancer Center, MCG, Augusta, GA

[2] H. Lee Moffitt Cancer Center, University of South Florida, 12902 Magnolia Drive, Tampa, FL 33612, USA

[3] Novartis Institute for Biomedical Research Inc., Cambridge, MA

Abstract

PURPOSE—Bortezomib (BZ) induces unfolded protein response (UPR) and endoplasmic reticulum (ER) stress, as well as exhibits clinical activity in patients with relapsed and refractory Mantle Cell Lymphoma (MCL). Here, we determined the molecular basis of the improved in vitro and in vivo activity of the combination of pan-histone deacetylase (HDAC) inhibitor (HDI) panobinostat (PS) and BZ against human, cultured and primary MCL cells.

EXPERIMENTAL DESIGN—Immunoblot analyses, RT-PCR and immunofluorescent and electron microscopy were utilized to determine the effects of PS on BZ-induced aggresome formation and ER stress in MCL cells.

RESULTS—Treatment with PS treatment induced heat shock protein (hsp) 90 acetylation, depleted the levels of hsp90 client proteins, CDK4, c-RAF and AKT, as well as abrogated BZ-induced aggresome formation in MCL cells. PS also induced lethal UPR, associated with induction of CHOP. Conversely, knockdown of CHOP attenuated PS-induced cell death of MCL cells. Compared to each agent alone, co-treatment with PS increased BZ-induced CHOP and NOXA expressions, as well as increased BZ-induced UPR and apoptosis of cultured and primary MCL cells. Co-treatment with PS also increased BZ-mediated in vivo tumor growth inhibition and improved survival of mice bearing human Z138C MCL cell xenograft.

CONCLUSION—These findings suggest that increased UPR and induction of CHOP are involved in enhanced anti-MCL activity of the combination of PS and BZ.

Keywords

Panobinostat; ER stress; MCL; Bortezomib; CHOP

Introduction

MCL is an aggressive, well-defined subset of B-cell non-Hodgkin's lymphoma (NHL), which accounts for nearly 6% of all lymphoma (1,2). It is characterized by deregulated expression of

Address correspondence to: Kapil N. Bhalla, M.D, Medical College of Georgia Cancer Center, 1120 15th street, CN2134, Augusta, Georgia 30912, Phone: 706-721-0463; Fax: 706-721-0469; kbhalla@mcg.edu.

Cyclin D1, due to the CCND1-IgH translocation, resulting from the chromosomal translocation t(11;14)(q13;q32) (2,3). In addition, MCL is often associated with expression of a truncated Cyclin D1 variant, enhanced activity of NFκB and AP1, genomic amplification of the cyclin-dependent kinase (CDK)-4, deletions of the CDK inhibitor p16INK4a, as well as overexpression of BMI-1, a transcriptional repressor of the p16INK4a locus (2,3). MCL patients respond initially to chemotherapy and autologous stem cell transplantation with an overall survival of about 3–4 years (4). However, after an initial response, a relapse is typical and chemoresistance is common (4). Several recent studies have documented clinical responses and benefit in MCL following treatment with a variety of novel agents. These include the mTOR kinase inhibitor temsirolimus, proteasome inhibitor bortezomib (BZ) and the immunomodulatory agent lenalidomide (4–6). However, none of these agents provide long term benefit and patients eventually succumb to the disease (4). These factors clearly indicate the necessity to develop novel combination therapies for the treatment of MCL.

BZ is a clinically effective agent in relapsed and refractory MCL (6). BZ exerts its anti-MCL activity through multiple mechanisms (7,8). These include inhibition of NFκB, stabilization of p53, generation of reactive oxygen species (ROS), induction of the BH3 domain-only protein NOXA, accumulation of misfolded proteins, as well as induction of protracted and lethal ER stress (7–9). Recently, pan-histone deacetylase (HDAC) inhibitors (HDIs), e.g., vorinostat and panobinostat (PS), were also documented to have clinical activity against a variety of hematological malignancies (10–12). HDI treatment induces cell cycle growth arrest and apoptosis of transformed more than normal cells through multiple mechanisms (13). For example, treatment with PS has been shown to increase ROS production, suppress Cyclin D1, induce cell cycle dependent kinase inhibitors p21 and p27, as well as induce the levels of the pro-apoptotic proteins, e.g., BAX, BAK and BIM in leukemia and other transformed cell types (13,14). Further, in some transformed cells, HDI treatment is known to decrease the levels of anti-apoptotic proteins, e.g., Bcl-xL, MCL-1, XIAP, survivin and AKT, thereby lowering the threshold for apoptosis (13,14). In previous reports, treatment with PS was demonstrated to inhibit HDAC6, induce heat shock protein (hsp) 90 acetylation, and disrupt chaperone association of hsp90 with its client proteins, including AKT, CDK4 and c-RAF, thereby promoting misfolding, polyubiquitylation and proteasomal degradation of the hsp90 client proteins (15–17). By inhibiting HDAC6, HDI treatment also abrogates formation of aggresome, which normally serves to sequester and protect against misfolded polyubiquitylated proteins (18). Consistent with this, HDI treatment has been shown to induce unfolded protein response (UPR) and ER stress (19). Disruption of ER homeostasis and the resulting proteotoxicity has been recognized as a novel mechanism for inhibiting tumor cell proliferation and survival, especially in B cell malignancies (20,21). Typically, UPR is an adaptive response to misfolded proteins in the ER which activates the ER membrane-bound mediators of ER stress response, IRE1 (Inositol Requiring Enzyme), PERK (PKR-like ER kinase) and ATF6α (Activated Transcription Factor α) (22,23). Accumulation of misfolded proteins causes the dissociation of the ER chaperone GRP (Glucose-regulated protein) 78 from the mediators of ER stress response, leading to their activation, with ensuing upregulation of gene expressions involved in either the alleviation of ER stress or cell death (22–24). UPR induces PERK-mediated phosphorylation of eIF2α (eukaryotic initiation factor), which blocks cap-dependent protein translation but allows preferential translation of ATF4, a transcription factor that up-regulates chaperone proteins required to restore ER function and induces the pro-death transcriptional regulator CHOP (22–24). CHOP is composed of an N-terminal transactivating domain and a C-terminal basic-leucine zipper (bZIP) domain. It functions by heterodimerizing with the C/EBP family of proteins and inhibiting their DNA binding or by binding to an alternate unique site to activate target genes (22–24). ATF6 activation leads to upregulation of genes that have an ER stress response element (ERSE) in their promoters such as GRP78, GRP94, CHOP and XBP1 (X-box binding protein 1) (22–24). Activated IRE1 catalyses the splicing of XBP1 to generate a frame-shift splice variant of XBP1 called XBP1s,

which induces GRP78 and other proteins involved in restoring normal ER function (22–24). However, persistent proteotoxic stress with unresolved UPR and ER stress results in protracted PERK signaling and CHOP mediated cell death (23–25). Consistent with this, combined treatment with BZ and an hsp90 inhibitor, which enhances UPR, has been shown to induce synergistic lethal effects in B cell malignancies (26). In present study, we determined the molecular basis of PS-mediated potentiation of BZ-induced UPR and ER stress resulting in lethal effects in cultured and primary MCL cells. Our findings demonstrate that, by inducing acetylation and inhibition of hsp90 chaperone function and concomitantly abrogating BZ-induced aggresome formation, PS accentuates BZ-induced UPR and ER stress in MCL cells. This is associated with increased CHOP expression due to co-treatment with PS and BZ, resulting in synergistic in vitro and in vivo cytotoxicity against human MCL cells. Our findings also demonstrate that CHOP knockdown inhibits PS-mediated cell death of MCL cells.

Materials and methods

Reagents and Antibodies

Panobinostat was provided by Novartis Pharmaceuticals Inc. (East Hanover, NJ). Phosho-eIF2α, eIF2α, Cyclin D1, AKT, Bak and PUMA were purchased from Cell Signaling Technology (Beverly, MA). CDK4, HDAC6, GRP78, Cyclin D1, c-Myc, Bax, ATF4 and CHOP antibodies were purchased from Santa Cruz Biotechnology, Inc., (Santa Cruz, CA). Monoclonal hsp90 antibodies were obtained from Assay Designs, MI. Anti-acetylated lysine, eIF2α, phospho-eIF2α and Bak antibodies were purchased from Cell Signaling technology (Beverly, MA). NOXA antibody was obtained from Abcam (Cambridge, MA), c-RAF antibodies were purchased from BD Transduction Laboratories (NJ, USA) and ubiquitin antibodies were obtained from Covance (Madison, WI).

MCL Cell lines and Primary MCL cells

Human MCL cell lines JeKo-1 and Z138C were obtained from ATCC and cultured in RPMI-1640 medium containing 20% heat-inactivated FBS. MO2058 cells were cultured as previously described (26). Granta-519 cells were obtained from DSMZ (Braunschweig, Germany) and cultured in DMEM containing 20% FBS. Logarithmically growing cells were exposed to the designated concentrations and exposure interval of the drugs. Following these treatments, cells were pelleted and washed free of the drug(s) prior to the performance of the studies described below. Primary MCL cells were obtained with informed consent as part of a clinical protocol approved by the Institutional Review Board of the Medical College of Georgia. Bone marrow and/or peripheral blood samples were collected in heparinized tubes and mononuclear cells were separated using Lymphoprep (Axis-Shield, Oslo, Norway), washed once in complete RPMI-1640 media, re-suspended in complete RPMI-media and counted to determine the number of isolated cells prior to their use in experiments. Percent cell death of primary MCL cells following 48 hours of exposure to PS and BZ was assessed in triplicates by trypan blue dye exclusion assay and a hemocytometer. Values are presented as percent cell death ± standard deviation.

Western Blot Analyses and immunoprecipitation

Western blot analyses were performed using specific anti-sera or monoclonal antibodies as described previously (14–16). The expression of β-actin was used as a loading control in immunoblot analyses. Data presented are representative of at least three independent experiments. Following drug treatments, cell lysates were incubated with 2 μg of hsp90 antibody was immunoprecipitated as previously described and probed with anti-acetyl lysine antibody to assess hsp90 acetylation. Immunoprecipitated hsp90 was detected by stripping the blot and immunoblotting with an hsp90 antibody (14–16). Horizontal scanning densitometry was performed on Western blots by using acquisition into Adobe PhotoShop (Adobe Systems

Inc., San Jose, CA) and analysis by the NIH Image Program (U.S. National Institutes of Health, Bethesda, MD).

ATP binding assay

MCL cells were incubated with indicated doses of PS for 16 hrs and washed free of drugs. ATP-bound proteins were immunoprecipitated from the resulting cell lysates by incubating with ATP-sepharose (Innova Bisociences, Cambridge, UK) beads for 4 hours. Following four washes, ATP-bound proteins were boiled with SDS-loading buffer and resolved on a 10% SDS PAGE gel. ATP-bound hsp90 was detected by immunoblotting with anti hsp90 antibody (Assay Designs, MI) (15).

Reverse transcription and Polymerase chain reaction (RT-PCR)

Total RNA was isolated from JeKo-1 cells and primary MCL cells using Trizol reagent (Invitrogen, Carlsbad, CA) as per manufacturer's instructions. Reverse transcription was performed with 2μg RNA using Supercript RT (Invitrogen, Carlsbad, CA). PCR reactions were performed using the corresponding specific primers listed below using 2X IQ Supermix (Biorad, Hercules, CA) reagent. The identity of PCR products was confirmed by sequencing. β-actin was used as a loading control. The authenticity of all PCR products was confirmed by sequencing.

XBP1s:

Forward primer 5′-TCTGCTGAGTCCGCAGCAG-3′

Reverse primer 5′-GAAAAGGGAGGCTGGTAAGGAAC-3′

XBP1u:

Forward primer 5′-GAGATGTTCTGGAGGGGTGACAAGTG-3′

Reverse primer 5′-TGGTTGCTGAAGAGGAGGCGGAAG-3′

ERdj4:

Forward primer 5′-GGTTCCAGTAGACAAAGGCATC-3′

Reverse primer 5′-GGTGATATTAGTGAGCCCAAGG-3′

CHOP:

Forward primer 5′-AAAATCAGAGCTGGAACCTGAG-3′

Reverse primer 5′-CCACTTTCCTTTCATTCTCCTG-3′

NOXA:

Forward primer 5′-CTCCTTCAAAAGAGTTTTCTCAGG-3′

Reverse primer 5′-CCCCAAGTAACCCTCCTATACTTT-3′

GADD34:

Forward primer 5′-CAGTGAAGAGGAGAGTGAG-3′

Reverse primer 5′-ACTTCAAGAAGACACCTGTAGC-3′

ERO-1α:

Forward primer 5′-GAATCTCTGAGTGAGGAAACAC-3′

Reverse primer 5′-TCTACACAGAGACCTTCTAGCC-3′

Confocal microscopy

MCL cells were incubated with indicated doses of drugs and cytospun onto slides. Following this they were fixed with 4% paraformaldehyde for 10 minutes, washed, permeabilized with 0.5% Triton-PBS buffer for 5 minutes and stained with HDAC6 and Ubiquitin antibodies as described previously (16). The images were visualized using Carl Zeiss LSM-510 meta confocal microscope with a 63X/1.2W objective.

Ultrastructural studies

MCL cells were exposed to BZ and/or PS for 16 hours. For transmission electron microscopy, MCL cells were fixed in 2% glutaraldehyde postfixed in 2% osmium tetroxide, stained en bloc with 2% uranyl acetate, dehydrated with a graded ethanol series and embedded in Epon-Araldite resin. Thin sections were cut with a diamond knife on a Leica EM UC6 ultramicrotome (Leica Microsystems, Inc, Bannockburn, IL), collected on copper grids and stained with uranyl acetate and lead citrate. Cells were observed in a JEM 1230 transmission electron microscope (JEOL USA Inc., Peabody, MA) at 80 kV and imaged with an UltraScan 4000 CCD camera and First Light Digital Camera Controller (Gatan Inc., Pleasanton, CA).

Tubulin deacetylase activity

Recombinant HDAC6 (Bio Vision, Mountain view CA) was incubated with equal concentrations of tubulin deacetylase (TDAC) substrate (Biomol International, L.P., PA) and increasing concentrations of panobinostat for 30 min in HDAC assay buffer (Biomol International, L.P., PA). Following this, the samples were incubated with Fluor de Lys developer and the fluorescent intensity was measured using a fluorimeter from BioTek Instruments Inc. (Winooski, VT). Inhibition of HDAC6 activity was expressed as percentage of untreated control values.

Annexin V- Propidium Iodide staining

MCL cell lines were exposed to indicated concentrations of drugs for 48 hours and pelleted down. Following washes with PBS, they were stained with Annexin-V FITC (BD Biosciences, NJ) and propidium iodide. Apoptotic cells were assessed using a FacsCalibur flow cytometer as described previously (14–16). Synergistic interactions were assessed using the median dose effect of Chou-Talalay. Combination indices (CI) for the two drugs were obtained using the commercially available software Calcusyn (Biosoft, Ferguson, MO) (26).

Transfection

JeKo-1 cells were transiently transfected using Turbofectin 8.0 (Origene, MD) as per manufacturers instructions, with the 3 μg plasmid vector pBS/U6 with or without the HDAC6 siRNA (15), which had a 21-nucleotide sequence 5′ GG ATG GAT CTG AAC CTT GAG A 3′, corresponding to the targeted nucleotides 200–219 in the HDAC6 mRNA (Accession # BC013737)

Retro viral knockdown of CHOP

siRNA to knockdown CHOP mRNA was designed using siRNA Target finder software (Ambion Inc., Austin, Tx). Oligonucleotides were denatured, annealed and cloned into pSilencer 5.1 H1 Retro vector using the BamHI and Hind III restriction sequences. The sequence of the siRNA duplex used in the study is as follows:

Sense strand siRNA: CCAGGAAACGGAAACAGAGtt

Antisense strand siRNA: CUCUGUUUCCGUUUCCUGGtt

Retrovirus production and retroviral infection

HEK-GP2 (host) cells were co-transfected with VSV-G (envelope protein) and pSilencer 5.1 H1 carrying scrambled oligos (control siRNA) or siCHOP oligos using Cal-Phos transfection reagent from Clontech (Mountain View, CA). Two days after transfection, the culture supernatants carrying retro viral particles were used for infecting JeKo-1 cells.

In vivo studies with MCL cells xenograft

Five million Z138C cells were implanted into the flanks of non-obese diabetic/severe combined immunodeficient (NOD-SCID) mice sub-cutaneously. Mice were divided into four groups (n=8). Tumors were allowed to grow and the treatment was commenced when the average tumor volume reached 50 mm^3. Control mice received DMSO. PS was administered at a dose of 10 mg/kg three times a week (Day 1, Day 3 and Day 5). BZ was administered at a dose of 0.5 mg/kg once a week (Day 2). No drugs were administered on Day 6 and Day 7. Mice receiving the combination therapy received PS and BZ as cited above. Treatment was continued for three weeks and the tumor volumes and survival of mice were recorded for each group. Mice were humanely sacrificed when the tumor volume reached 2000 mm^3. The day of death was noted and plotted on a Kaplan-Meier plot as described previously (14).

Statistical Analyses

Data were expressed as mean ± standard deviation. Comparisons used student's t test or ANOVA, as appropriate. P values of < 0.05 were assigned significance.

Results

Panobinostat induces hyperacetylation and inhibition of hsp90 in MCL cells

First we confirmed whether panobinostat inhibits HDAC6 and induces hyperacetylation of hsp90 in MCL cells, as has been described in human leukemia cells (15). Figure 1A demonstrates that treatment with panobinostat (20 nM) inhibited the in vitro activity of recombinant HDAC6 by greater than 90% in a cell-free assay, which was only slightly augmented following exposure to 50 nM panobinostat (Figure 1A). Treatment with PS, or knockdown of HDAC6 with siRNA, also induced hyperacetylation of hsp90 in JeKo-1 cells, indicative of intracellular inhibition of HDAC6 (Figure 1B). This was further substantiated by the notable induction of α-tubulin acetylation in PS-treated Jeko-1 cells (data not shown) (15,16). PS-induced hyperacetylation of hsp90 was associated with decreased binding of ATP to hsp90, which was previously reported by us to undermine the chaperone function of hsp90 (Figure 1C) (15). Consequently, treatment with PS results in an increase in the levels of misfolded, polyubiquitylated hsp90 client proteins (15). Similarly, treatment with BZ inhibits the degradation of misfolded polyubiquitylated proteins by the proteasomes (18). Therefore, we determined the levels of polyubiquitylated proteins in JeKo-1 cell lysates treated with PS and BZ. Although not as much as that following an exposure to 20 nM of BZ, PS (20 nM) also resulted in accumulation of polyubiquitylated, especially high molecular weight, proteins in MCL cells (Figure 1D). Collectively, these findings indicate that PS-mediated hyeperacetylation and inhibition of hsp90 leads to increased levels of polyubiquitylated proteins.

Panobinostat abrogates Bortezomib-induced aggresome formation in MCL cells

HDAC6 has been shown to bind and sequester intracellular polyubiquitylated proteins into aggresome, which is a perinuclear organelle formed as a protective response against proteotoxic stress, e.g., induced by the proteasome inhibitor BZ (18). Therefore, we determined the effect of PS on BZ-induced aggresome formation in MCL cells, utilizing immunofluorescent and electron microscopy. As shown in Figure 2A and 2B, treatment of

JeKo-1 and Granta-519 cells with BZ led to formation of aggresome in up to 30–35% cells (Figure 2A and 2B). Co-treatment with PS abrogated BZ-induced aggresome formation (Figure 2A and 2B) ($p \leq 0.005$ for BZ treatment versus the co-treatment). Similar effects were observed following treatment with tubacin (5.0 μM), which is a relatively specific but weak inhibitor of HDAC6 (data not shown). Transmission electron microscopy of JeKo-1 cells following exposure to BZ revealed the presence of electron-dense perinuclear aggresome (Figure 2C), lacking a membrane envelope and surrounded by mitochondria (28). PS treatment alone induced ER dilatation in JeKo-1 cells, indicative of ER stress, while combined treatment with PS and BZ induced highly dilated ER and partial dissolution of the nuclear envelope (arrowhead) (Figure 2C and inset). This indicated the induction of a more profound ER stress. These data clearly show for the first time that treatment with PS inhibits BZ-induced aggresome formation in human MCL cells.

Panobinostat depletes hsp90 client proteins as well as induces ER stress and apoptosis in MCL cells

Following PS treatment, induction of ER stress in MCL cells was demonstrated by the induction of the mRNA and protein markers of ER stress. Treatment of JeKo-1 and Z138C cells with PS induced XBP1s, Erdj4 (an ER homolog of hsp40 and a downstream target of XBP1s) and NOXA mRNA was more in JeKo-1 cells than Z138C cells. CHOP mRNA was induced in both Z138C and JeKo-1 cells (Figure 3A). Additionally, PS treatment resulted in increased expression of CHOP, ATF4 and GRP78 in JeKo-1 and Z138C cells (Figure 3B). Treatment with PS led to a dose-dependent increase in apoptosis of JeKo-1, MO2058, Granta-519 and Z138C cells, as assessed by Annexin V and PI staining (Figure 3C). This was associated with PS-mediated depletion of hsp90 client proteins, including c-RAF, AKT, CDK4 and Cyclin D1 (15,17), as well as the induction of pro-apoptotic BAX and BAK and down regulation of survivin and c-Myc levels (Figure 3D) (29). These data show for the first time that treatment of MCL cells with clinically achievable concentration of PS leads to UPR, while simultaneously disrupting hsp90 chaperone function and depleting pro-survival and up-regulating pro-apoptotic proteins. Consistent with the previous reports, our studies also demonstrate that treatment with BZ dose-dependently induced apoptosis in MO2058, Z138C and JeKo-1 cells (Supplementary Figure 1A). This was associated with BZ-induced ER stress as evidenced by induction of mRNA of XBP1s and its transcriptional target Erdj4. BZ treatment also induced CHOP and NOXA mRNA levels (Supplementary Figures 1B).

Co-treatment with PS and BZ causes enhanced UPR in MCL cells

As suggested by the electron microscopy findings noted above, we next determined whether co-treatment with PS would increase BZ-induced molecular hallmarks of UPR and ER stress. As shown in Figure 4A, co-treatment with PS increased BZ-induced GRP78, CHOP and PUMA levels in JeKo-1 cells (Figure 4A). Increased CHOP induction was also associated with the up-regulation of the mRNA of another CHOP-inducible transcript, ER oxidase 1α (ERO-1α) Figure 4B). Importantly, increased CHOP levels, following combined treatment with PS and BZ, led to up-regulation of GADD34 expression, a CHOP-inducible phosphatase responsible for dephosphorylating eIF2α (Figure 4A) (23–25,30–32). This was associated with decreased phosphorylation of eIF2α following combined treatment with BZ and PS. As compared to treatment with each agent alone, co-treatment with PS and BZ induced synergistic apoptosis of Jeko-1 cells, as indicated by the combination indices of less then 1.0 by isobologram analysis (Figure 4C). Superior activity of the combination was also noted for Z138C cells (data not shown). Collectively, these observations also suggest that enhanced CHOP expression and ensuing CHOP-induced gene-products may contribute to the lethal effects of PS and BZ against MCL cells (Figure 4B & C).

Effect of knockdown of CHOP on the sensitivity of MCL cells to PS

We next determined the role of CHOP induction in the lethal UPR mediated by treatment with PS or BZ. Retroviral knockdown of CHOP by siRNA partially decreased the sensitivity of JeKo-1 cells to PS (p=0.001) (Figure 4D). In contrast, knockdown of CHOP only slightly decreased the sensitivity of JeKo-1 cells to BZ-induced cell death ($p > 0.05$; data not shown). The modest effects of CHOP knockdown on BZ-induced cell death may be because treatment with BZ engages multiple mechanisms of cell death in transformed cells (8). For example, BZ treatment also induces the pro-death BH3-only domain containing protein NOXA, as shown in Figure 4A. Collectively, these observations indicate that CHOP induction contributes to PS-induced lethal ER stress in MCL cells.

Co-treatment with BZ and PS exerted superior in vitro activity against primary MCL cells and in vivo activity in mice with Z138C xenograft

The lethal effects of co-treatment with PS and BZ were also determined against three samples of primary MCL cells (Table 1). As shown, each sample had different sensitivity to PS and BZ-mediated cell death, although co-treatment resulted in more cell death than treatment with each agent alone; $p \leq 0.05$ (Table 1). Due to inadequate number of cells in the MCL samples, full analysis of a synergistic effect of the combination could not be determined. However, as compared to the effect of PS or BZ alone, co-treatment with PS and BZ for 24 hours caused more induction of GRP78, Erdj4, CHOP and NOXA mRNA levels in the primary MCL samples (Figure 5). As compared to each agent alone, co-treatment with PS and BZ does not induce greater cell death or UPR in normal CD34+ bone marrow progenitor cells (Table 1 and Figure 5). To determine the in vivo effects of PS and/or BZ, Z138C MCL cells were subcutaneously implanted in the NOD-SCID mice. Tumors were allowed to grow until the average tumor volume reached 50 mm^3. The mice were treated with vehicle, or with the previously determined sub-maximally tolerated dose (MTD) dose of BZ (0.5 mg/kg once a week), PS (10 mg/kg three times a week), or the combination of the two drugs. Tumor volumes were recorded and the mice were humanely euthanized when the tumor volume reached 2000 mm^3. Following three weeks of treatment with PS and/or BZ, the mean tumor volumes were significantly lower in the mice treated with the combination, as compared to those treated with each drug alone ($p < 0.05$) (Figure 6A). Moreover, treatment with PS or the combination of BZ and PS demonstrated a significant increase in the survival of mice (p=0.05 and 0.001 respectively) as compared to treatment with BZ or vehicle alone (Figure 6B). Median survival of mice treated with PS and BZ was 47 days, compared to 41 and 37 days for the mice treated with PS or vehicle alone, respectively.

Discussion

Present studies demonstrate for the first time that in human MCL cells PS inhibits HDAC6, thereby inducing hyperacetylation and attenuation of hsp90 chaperone function (15–17). PS-mediated HDAC6 inhibition also increases the intracellular levels of polyubiquitylated proteins, since HDAC6 has been shown to regulate the accumulation of ubiquitylated, toxic protein aggregates and noted to be a cellular stress surveillance factor (33,34). While increasing the intracellular accumulation of misfolded proteins, treatment with PS simultaneously abrogates HDAC6-mediated aggresome formation, which is normally an adaptive and protective response-the first line of defense against misfolded proteins (18). Collectively, as underscored by these findings, PS-induced perturbations in protein triage result in UPR and ER stress in MCL cells. This is associated with increased levels of XBP1s, as well as activation of PERK and p-eIF2α. The latter is designed to reduce general protein synthesis, while concomitantly promoting protein folding through increased levels of the molecular chaperones, such as GRP78, as well as enhancing the ER associated protein degradation (ERAD) (22,23).

However, sustained exposure to PS and induction of CHOP leads to apoptosis, thus converting the protective and adaptive response to a lethal UPR in MCL cells.

The role of a maintenance or "physiological UPR" has been well-appreciated in B cell development and maturation. For instance, IRE1α has been reported to be crucial for B lymphopoiesis, IgG rearrangement and production of B cell receptors (BCR) (35). The induction of XBP1s mRNA is established as an important step in B-cell maturation into plasma cells and XBP1s expression is known to drive multiple myeloma pathogenesis (36,37). Therefore, the significance of ER stress in B-cell development, maturation and function, also creates the rationale as to why transformed B cells might be especially susceptible to agents that accentuate the UPR, leading to protracted and lethal ER stress. This approach has been clinically validated and exemplified by the anti-MCL and anti-MM activity of BZ, which induces lethal UPR in the pre-clinical models of these malignancies (6,38). Present studies, however, show the mechanistic link between PS-mediated increased accumulation of polyubiquitylated proteins and HDAC6 inhibition and aggresome disruption to PS-mediated accentuation of BZ-induced proteotoxic stress and lethal UPR in human MCL cells. These findings are consistent with the previous reports demonstrating that in MM cells HDI treatment induced UPR, and co-treatment with PS further enhanced BZ-induced UPR and apoptosis of MM cells (38,39). Our results presented here show that co-treatment with BZ appears to further heighten the sensitivity of MCL cells to PS-induced aggresome dysfunction and heightened UPR. Catley et al reported a similar effect in MM cells (40). In MCL cells, as compared to treatment with PS or BZ alone, co-treatment with PS and BZ led to synergistic and lethal ER stress, as evidenced by ultrastructural changes showing dilated ER, as well as by increased levels of CHOP and NOXA. Previous studies have also documented a mechanistic role of increased CHOP and NOXA levels underlying lethal ER stress (30,41,42). Collectively, the significance of these findings is highlighted in the model presented in Figure 7. Furthermore, in support of the model, our findings demonstrate that knockdown of CHOP confers resistance to PS-induced cell death in MCL cells. In contrast, CHOP knockdown did not significantly reduce BZ-induced cell death. This may be because BZ activates multiple mechanisms and is consequently less dependent on CHOP in mediating its lethal effects in MCL cells (8). Although not seen in the cultured MCL cells used in the present studies, increased BIM levels have also been shown to mediate the lethal outcome of UPR (43).

Our findings also demonstrate that, in MCL cells, in addition to upregulating pro-death proteins, PS-mediated hyperacetylation of hsp90 and attenuation of hsp90 chaperone function, is also associated with depletion of important pro-growth and pro-survival, MCL-relevant onco-client proteins, including cyclin D1, CDK4, MYC, AKT and c-RAF. Most likely, this also lowers the threshold for apoptosis in MCL cells (17,29). Additionally, in previous studies both PS and BZ have been shown to induce reactive oxygen species (ROS), which may contribute to the cytotoxicity of the combination in MCL cells (7,8,14). The synergism observed with the combination of HDAC inhibitors and BZ could also be, at least partly, because of inhibition of NF-κB induction by BZ since treatment with PS alone is known to induce NF-κB, which may exert an anti-apoptotic effect (44). Taken together, these observations indicate that in addition to lethal UPR, other mechanisms may be involved in the observed synergistic activity of PS and BZ in MCL cells, as is proposed in the model presented in Figure 7. The combination of PS and BZ also appears to hasten the in-built negative feedback mechanism in UPR to dephosphorylate eIF2α by inducing GADD34 (31,32). This is probably a direct consequence of CHOP up-regulation and activation of its downstream target GADD34 or the stabilization of GADD34 by proteasome inhibition (31,32,45).

Results presented here show that as compared to each agent alone, the combination of PS and BZ also showed superior activity against primary MCL cells. Although full evaluation of the molecular correlates of this superior activity was not feasible, its molecular correlates included

induction of mRNA levels of CHOP and NOXA, suggesting increased and lethal ER stress in the primary MCL cells. More complete analyses of the effects of PS and BZ has to be conducted before any firm conclusions can be drawn about the degree of superior activity and about the predictive biomarkers of response to the combination. Co-treatment with PS and BZ also resulted in increased tumor growth delay and survival in a mouse xenograft model of human MCL cells. Recently, results of a phase I study of a combination of vorinostat and BZ showed that the combination of drugs belonging to these two classes of agents is clinically feasible and demonstrates promising clinical activity in BZ refractory MM (46). Supported by our pre-clinical in vitro and in vivo findings presented here, the results of this trial support the rationale for testing the combination of PS and BZ in patients with MCL.

Statement of Translational Relevance

Although treatment with the proteasome inhibitor bortezomib has shown promise against refractory and relapsed MCL, none of the therapies for MCL, including bortezomib, induce long term remission. Therefore, there is a need to develop effective combination therapies for MCL. In view of these observations, we tested the anti-MCL activity of the combination of panobinostat and bortezomib against human MCL cells. Our data indicate that panobinostat increases intracellular ubiquitylated proteins, inhibits aggresome formation and induces lethal unfolded protein response (UPR) in MCL cell. Co-treatment with panobinostat enhanced bortezomib-induced lethal ER stress, leading to synergistic in vitro and superior in vivo anti-tumor activity of the combination against human MCL cells. These observations support the rationale to further evaluate the in vivo efficacy of co-treatment with panobinostat and bortezomib against human MCL.

Supplementary Material

Refer to Web version on PubMed Central for supplementary material.

References

1. Andersen NS, Jensen MK, de Nully Brown P, Geisler CH. A Danish population-based analysis of 105 mantle cell lymphoma patients: incidences, clinical features, response, survival and prognostic factors. Eur J Cancer 2002;38:401–08. [PubMed: 11818206]
2. Smith MR. Mantle cell lymphoma: advances in biology and therapy. Curr Opin Hematol 2008;15:415–21. [PubMed: 18536582]
3. Jares P, Colomer D, Campo E. Genetic and molecular pathogenesis of mantle cell lymphoma: perspectives for new targeted therapeutics. Nat Rev Cancer 2007;7:750–62. [PubMed: 17891190]
4. Schmidt C, Dreyling M. Therapy of mantle cell lymphoma: current standards and future strategies. Hematol Oncol Clin North Am 2008;22:953–63. ix. [PubMed: 18954745]
5. O'Connor OA. Mantle cell lymphoma: Identifying novel molecular targets in growth and survival pathways. Hematol/Educ Progr of the Amer Soc of Hematol 2007:270–76.
6. O'Connor OA, Moskowitz C, Portlock C, et al. Patients with chemotherapy-refractory mantle cell lymphoma experience high response rates and identical progression-free survivals compared with patients with relapsed disease following treatment with single agent bortezomib: results of a multicentre Phase 2 clinical trial. Brit J Hemat 2009;145:34–9.
7. Perez-Galan P, Roue G, Villamor N, Montserrat E, Campo E, Colomer D. The proteasome inhibitor bortezomib induces apoptosis in mantle-cell lymphoma through generation of ROS and Noxa activation independent of p53 status. Blood 2006;107:257–64. [PubMed: 16166592]
8. McConkey DJ, Zhu K. Mechanisms of proteasome inhibitor action and resistance in cancer. Drug Resist Updat 2008;11:164–79. [PubMed: 18818117]

9. Nawrocki ST, Carew JS, Dunner K Jr, et al. Bortezomib inhibits PKR-like endoplasmic reticulum (ER) kinase and induces apoptosis via ER stress in human pancreatic cancer cells. Cancer Res 2005;65:11510–519. [PubMed: 16357160]
10. Ottmann OG, Spencer A, Prince HM, et al. Phase IA/II Study of Oral Panobinostat (LBH589), a Novel Pan-Deacetylase Inhibitor (DACi) Demonstrating Efficacy in Patients with Advanced Hematologic Malignancies. Blood 2008:110. Abstract 958.
11. Duvic M, Talpur R, Ni X, et al. Phase 2 trial of oral vorinostat (suberoylanilide hydroxamic acid, SAHA) for refractory cutaneous T-cell lymphoma (CTCL). Blood 2007;109:31–9. [PubMed: 16960145]
12. Watanabe T, Kato H, Kobayashi Y, et al. Potential efficacy of the oral histone deacetylase inhibitor vorinostat in a phase I trial in follicular and mantle cell lymphoma. Cancer Sci 2009;101:196–200. [PubMed: 19817748]
13. Minucci S, Pelicci PG. Histone deacetylase inhibitors and the promise of epigenetic (and more) treatments for cancer. Nat Rev Cancer 2006;6:38–51. [PubMed: 16397526]
14. Fiskus W, Rao R, Fernandez P, Herger B, Yang Y, Chen J, Kolhe R, Mandawat A, Wang Y, Joshi R, Eaton K, Lee P, Atadja P, Peiper S, Bhalla K. Molecular and biologic characterization and drug-sensitivity of pan histone deacetylase inhibitor resistant acute myeloid leukemia cells. Blood 2008;112:2896–905. [PubMed: 18660379]
15. Bali P, Pranpat M, Bradner J, et al. Inhibition of histone deacetylase 6 acetylates and disrupts the chaperone function of heat shock protein 90: a novel basis for antileukemia activity of histone deacetylase inhibitors. J Biol Chem 2005;280:26729–734. [PubMed: 15937340]
16. Yang Y, Rao R, Shen J, et al. Role of acetylation and extracellular location of heat shock protein 90alpha in tumor cell invasion. Cancer Res 2008;68:4833–842. [PubMed: 18559531]
17. Pearl LH, Prodromou C, Workman P. The Hsp90 molecular chaperone: an open and shut case for treatment. Biochem J 2008;410:439–53. [PubMed: 18290764]
18. Kawaguchi Y, Kovacs JJ, McLaurin A, Vance JM, Ito A, Yao TP. The deacetylase HDAC6 regulates aggresome formation and cell viability in response to misfolded protein stress. Cell 2003;115:727–38. [PubMed: 14675537]
19. Park MA, Zhang G, Martin AP, et al. Vorinostat and sorafenib increase ER stress, autophagy and apoptosis via ceramide-dependent CD95 and PERK activation. Cancer Biol Ther 2008;7:1648–62. [PubMed: 18787411]
20. Hideshima T, Bradner JE, Wong J, et al. Small-molecule inhibition of proteasome and aggresome function induces synergistic antitumor activity in multiple myeloma. Proc Natl Acad Sci U S A 2005;102:8567–72. [PubMed: 15937109]
21. Davenport EL, Moore HE, Dunlop AS, Sharp SY, Workman P, Morgan GJ, et al. Heat shock protein inhibition is associated with activation of the unfolded protein response pathway in myeloma plasma cells. Blood 2007;110:2641–49. [PubMed: 17525289]
22. Szegezdi E, Logue SE, Gorman AM, Samali A. Mediators of endoplasmic reticulum stress-induced apoptosis. EMBO Rep 2006;7:880–85. [PubMed: 16953201]
23. Ron D, Walter P. Signal integration in the endoplasmic reticulum unfolded protein response. Nat Rev Mol Cell Biol 2007;8:519–29. [PubMed: 17565364]
24. Marciniak SJ, Yun CY, Oyadomari S, et al. CHOP induces death by promoting protein synthesis and oxidation in the stressed endoplasmic reticulum. Genes Dev 2004;18:3066–77. [PubMed: 15601821]
25. Lin JH, Li H, Yasumura D, et al. IRE1 signaling affects cell fate during the unfolded protein response. Science 2007;318:944–49. [PubMed: 17991856]
26. Rao R, Lee P, Fiskus W, et al. Co-treatment with heat shock protein 90 inhibitor 17-dimethylaminoethylamino-17-demethoxygeldanamycin (DMAG) and vorinostat: a highly active combination against human mantle cell lymphoma (MCL) cells. Cancer Biol & Ther 2009;8:1273–80. [PubMed: 19440035]
27. Lwin T, Hazlehurst LA, Dessureault S, et al. Cell adhesion induces p27Kip1-associated cell-cycle arrest through down-regulation of the SCFSkp2 ubiquitin ligase pathway in mantle-cell and other non-Hodgkin B-cell lymphomas. Blood 2007;110:1631–38. [PubMed: 17502456]
28. Johnston JA, Ward CL, Kopito RR. Aggresomes: a cellular response to misfolded proteins. J Cell Biol 1998;143:1883–98. [PubMed: 9864362]

29. Hotchkiss RS, Strasser A, McDunn JE, Swanson PE. Cell death. N Engl J Med 2009;361:1570–83. [PubMed: 19828534]
30. Lin JH, Li H, Zhang Y, Ron D, Walter P. Divergent effects of PERK and IRE1 signaling on cell viability. PLoS One 2009;4:e4170. [PubMed: 19137072]
31. Novoa I, Zeng H, Harding HP, Ron D. Feedback inhibition of the unfolded protein response by GADD34-mediated dephosphorylation of eIF2alpha. J Cell Biol 2001;153:1011–22. [PubMed: 11381086]
32. Novoa I, Zhang Y, Zeng H, Jungreis R, Harding HP, Ron D. Stress-induced gene expression requires programmed recovery from translational repression. EMBO J 2003;22:1180–87. [PubMed: 12606582]
33. Boyault C, Zhang Y, Fritah S, et al. HDAC6 controls major cell response pathways to cytotoxic accumulation of protein aggregates. Genes Dev 2007;21:2172–81. [PubMed: 17785525]
34. Matthias P, Yoshida M, Khochbin S. HDAC6 a new cellular stress surveillance factor. Cell Cycle 2008;7:7–10. [PubMed: 18196966]
35. Zhang K, Wong HN, Song B, Miller CN, Scheuner D, Kaufman RJ. The unfolded protein response sensor IRE1alpha is required at 2 distinct steps in B cell lymphopoiesis. J Clin Invest 2005;115:268–81. [PubMed: 15690081]
36. Reimold AM, Iwakoshi NN, Manis J, et al. Plasma cell differentiation requires the transcription factor XBP-1. Nature 2001;412:300–07. [PubMed: 11460154]
37. Carrasco DR, Sukhdeo K, Protopopova M, et al. The differentiation and stress response factor XBP-1 drives multiple myeloma pathogenesis. Cancer Cell 2007;11:349–60. [PubMed: 17418411]
38. Laubach JP, Mahindra A, Mitsiades CS, et al. The use of novel agents in the treatment of relapsed and refractory multiple myeloma. Leukemia 2009;23:2222–32. [PubMed: 19741729]
39. Mitsiades CS, Hideshima T, Chauhan D, et al. Emerging treatments for multiple myeloma: beyond immunomodulatory drugs and bortezomib. Semin Hematol 2009;46:166–75. [PubMed: 19389500]
40. Catley L, Weisberg E, Kiziltepe T, et al. Aggresome induction by proteasome inhibitor bortezomib and alpha-tubulin hyperacetylation by tubulin deacetylase (TDAC) inhibitor LBH589 are synergistic in myeloma cells. Blood 2006;108:3441–49. [PubMed: 16728695]
41. Nawrocki ST, Carew JS, Maclean KH, et al. Myc regulates aggresome formation, the induction of Noxa, and apoptosis in response to the combination of bortezomib and SAHA. Blood 2008;112:2917–26. [PubMed: 18641367]
42. Wang Q, Mora-Jensen H, Weniger MA, et al. ERAD inhibitors integrate ER stress with an epigenetic mechanism to activate BH3-only protein NOXA in cancer cells. Proc Natl Acad Sci U S A 2009;106:2200–05. [PubMed: 19164757]
43. Puthalakath H, O'Reilly LA, Gunn P. ER stress triggers apoptosis by activating BH3-only protein Bim. Cell 2007;129:1337–49. [PubMed: 17604722]
44. Dai Y, Chen S, Kramer LB, Funk VL, Dent P, Grant S. Interactions between bortezomib and romidepsin and belinostat in chronic lymphocytic leukemia cells. Clin Cancer Res 2009;14:549–58. [PubMed: 18223231]
45. Brush MH, Shenolikar S. Control of cellular GADD34 levels by the 26S proteasome. Mol Cell Biol 2008;28:6989–7000. [PubMed: 18794359]
46. Badros A, Burger AM, Philip S, et al. Phase I study of vorinostat in combination with bortezomib for relapsed and refractory multiple myeloma. Clin Cancer Res 2009;15:5250–57. [PubMed: 19671864]

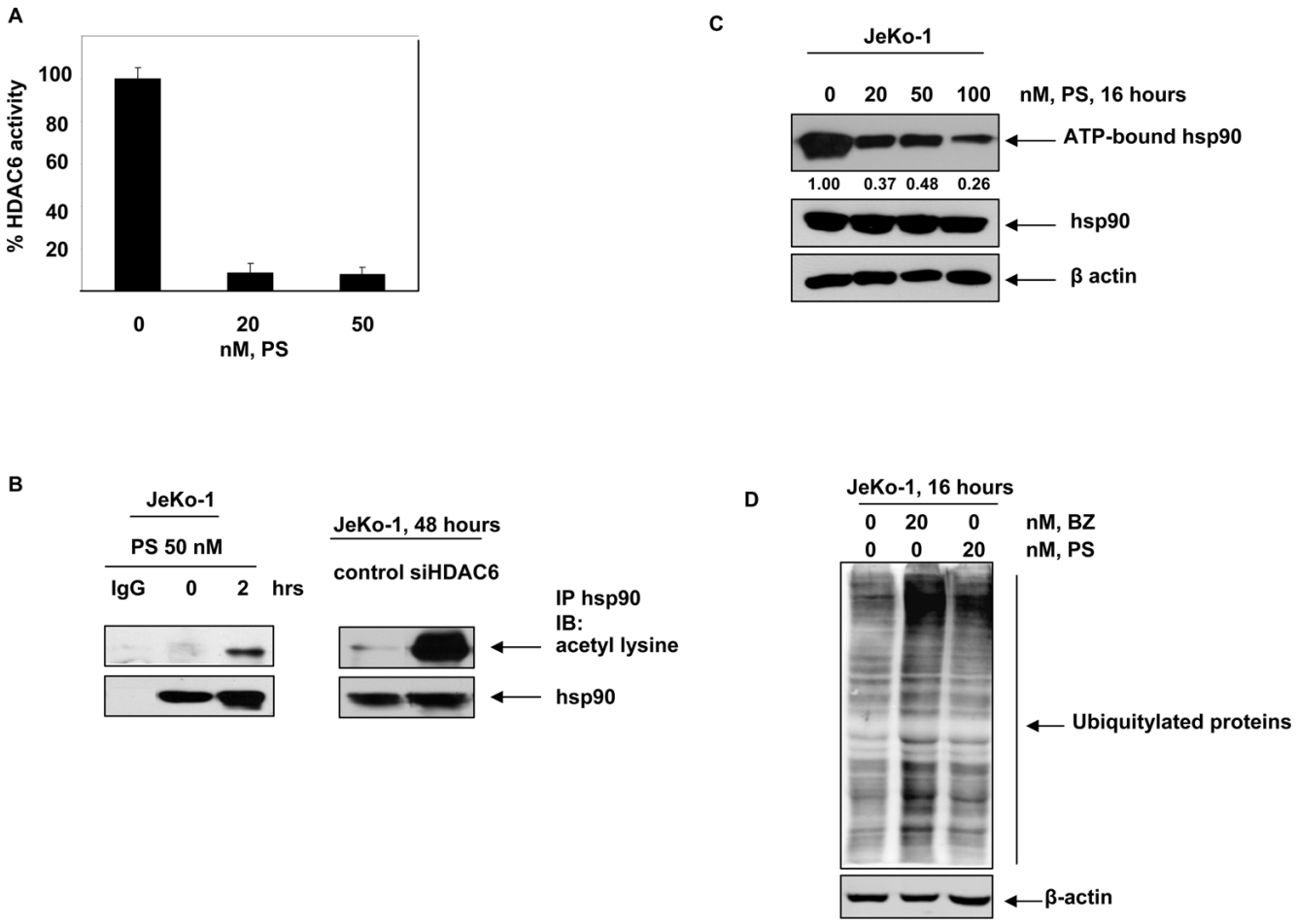

Figure 1. Panobinostat induces apoptosis and abrogates hsp90 chaperone function in MCL cells

A, Recombinant HDAC6 was incubated in vitro with indicated doses of PS and the tubulin deacetylase activity of HDAC6 was monitored. Percent reduction in HDAC6 activity is plotted as a function of increasing doses of PS. **B**, JeKo-1 cells were treated with 50 nM, PS for 2 hours and hsp90 was immunoprecipitated from the cells. Acetylation of hsp90 was assessed by immunoblotting with acetyl-lysine antibodies. Alternatively, JeKo-1 cells were transfected with vector or siHDAC6 plasmids and the acetylation of hsp90 was monitored 48 hours later. **C**, JeKo-1 cells were incubated with indicated doses of PS for 16 hrs and ATP-bound proteins were immunoprecipitated using ATP-sepharose. Hsp90 in the complex was assessed by immunoblotting for hsp90. **D**, JeKo-1 cells were treated with PS and BZ for 16 hours and the accumulation of polyubiquitylated proteins was assessed by immunoblotting for ubiquitin.

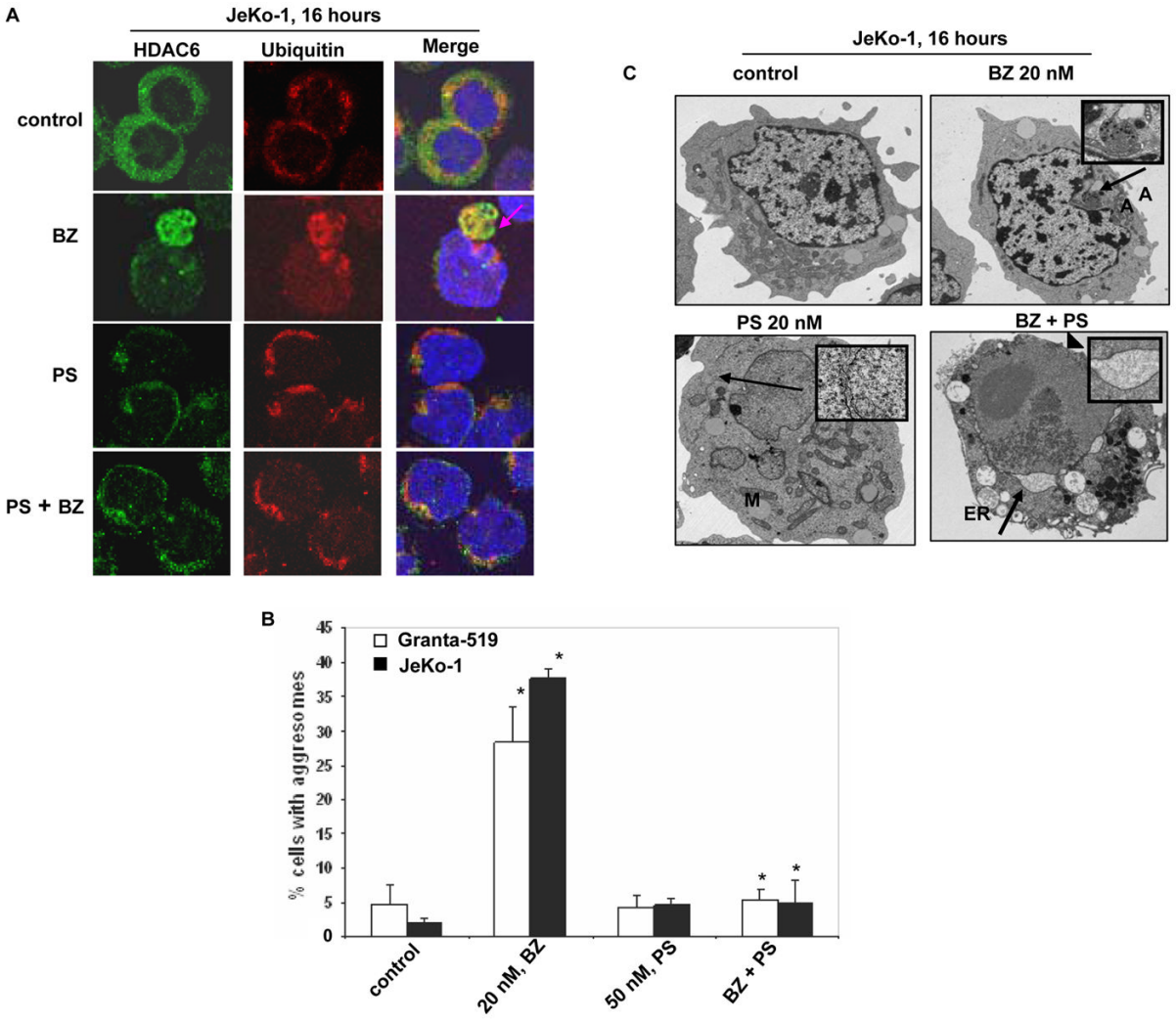

Figure 2. Panobinostat abrogates bortezomib-induced aggresome formation in JeKo-1 and Granta-519 cells

A, JeKo-1 cells were treated with BZ, PS and a combination of the two for 16 hours and stained for HDAC6 and ubiquitin. Following this, immunofluroescent microscopy was performed using LSM-510 confocal microscope using a 63X/1.2 W correction objective. **B**, JeKo-1 and Granta-519 cells were treated with BZ, PS or a combination of the two drugs and the percentage of cells with aggresomes were counted. Values were plotted as the percentage of aggresome positive cells ± standard deviation. The p value for BZ versus the co-treatment is less than or equal to 0.005. **C**, JeKo-1 cells were treated with indicated doses of PS and BZ and the ultrastructure of cells was imaged using a transmission electron microscope. Aggresomes and ER dilatation are indicated by arrows and depicted as insets.

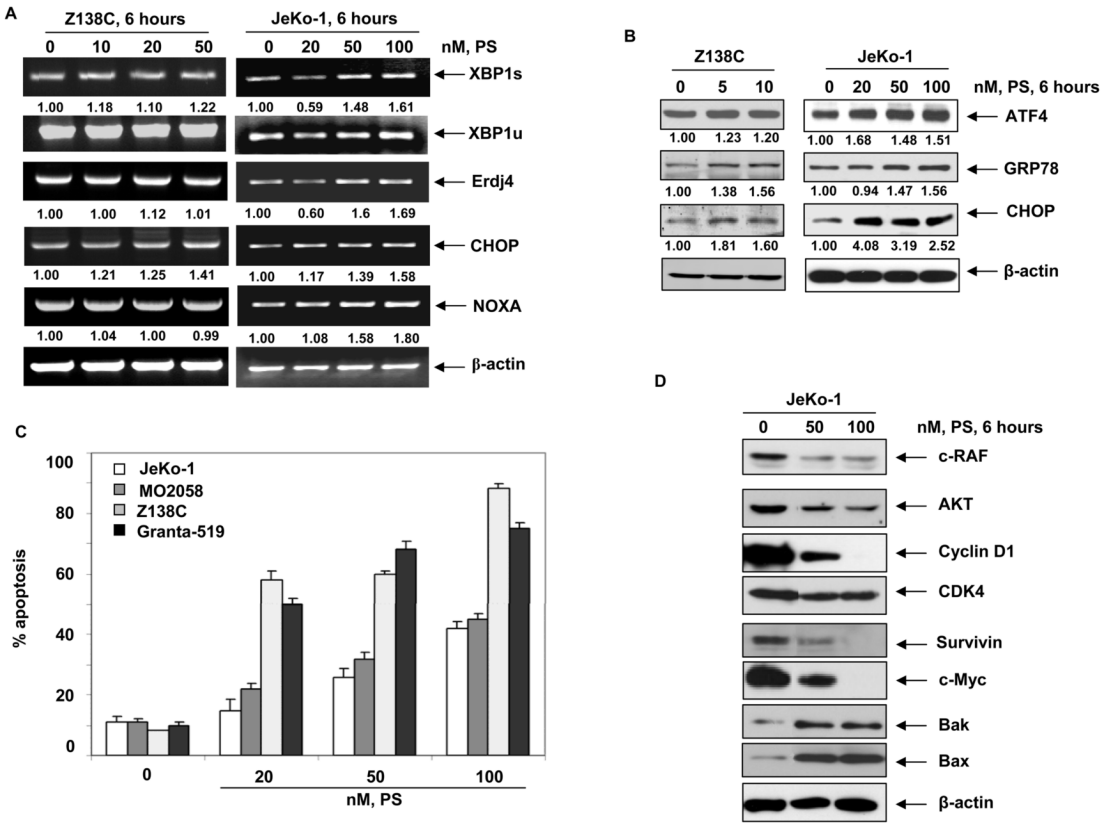

Figure 3. Treatment with Panobinostat induces ER stress, results in dose-dependent apoptosis and abrogates hsp90 client proteins in MCL cells

A, JeKo-1 and Z18C cells were treated with indicated doses of PS for 6 hours and the mRNA expression of XBP1s, XBP1u, Erdj4, CHOP and NOXA was assessed by RT-PCR. The expression of β-actin served as a loading control. **B**, JeKo-1 and Z138C cells were treated with indicated doses of PS for 6 hours and the expression of ATF4, GRP78 and CHOP was assessed by immunoblotting. **C**, JeKo-1, MO2058, Z138C and Granta-519 cells were exposed to the indicated doses of PS for 48 hours and apoptosis was monitored by Annexin V and PI staining followed by flow cytometry. **D**, JeKo-1 cells were exposed to indicated doses of PS for 6 hours and the expression of c-RAF, AKT, Cyclin D1, CDK, survivin, c-Myc, BAK, BAX and β-actin were monitored by immunoblot analyses.

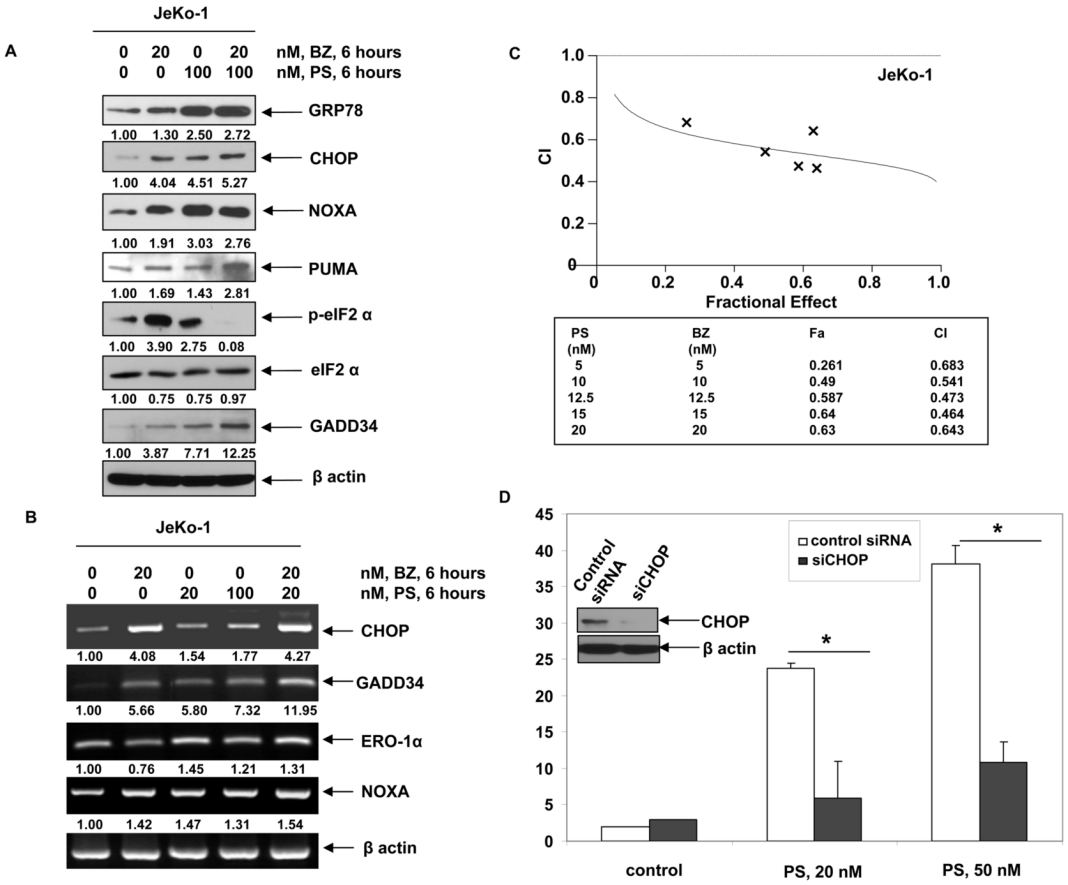

Figure 4. Co-treatment of MCL cells with bortezomib and Panobinostat induces enhanced ER stress in MCL cells

A, JeKo-1 cells were treated with indicated doses of PS and/or BZ for 6 hours and the expression of GRP78, CHOP, NOXA, PUMA, p-eIF2α, eIF2α, and GADD34 was assessed by immunoblot analysis. **B**, Alternatively, the expression of CHOP, GADD34, ERO-1α, NOXA and β-actin mRNA was assessed by RT-PCR following 6 hours of exposure of JeKo-1 cells to BZ and PS. **C**, JeKo-1 cells were treated with PS and BZ at a 1:1 molar ratio stained for Annexin V-PI. Percentage of apoptotic cells was assessed by flow cytometry. The combination index (CI) for each treatment was determined using Calcusyn software. CI values of less than 1.0 represent synergistic interactions. **D,** JeKo-1 cells were infected with retroviral scrambled siRNA or CHOP siRNA and treated with PS following 48 hours of infection. Viability of cells following CHOP knockdown and 24 hours of exposure to PS was assessed by trypan blue dye exclusion assay and a hemocytometer. Values presented are an average of three independent experiments ± standard deviation. Inset shows immunoblot analysis of CHOP protein after 48 hours of infection.

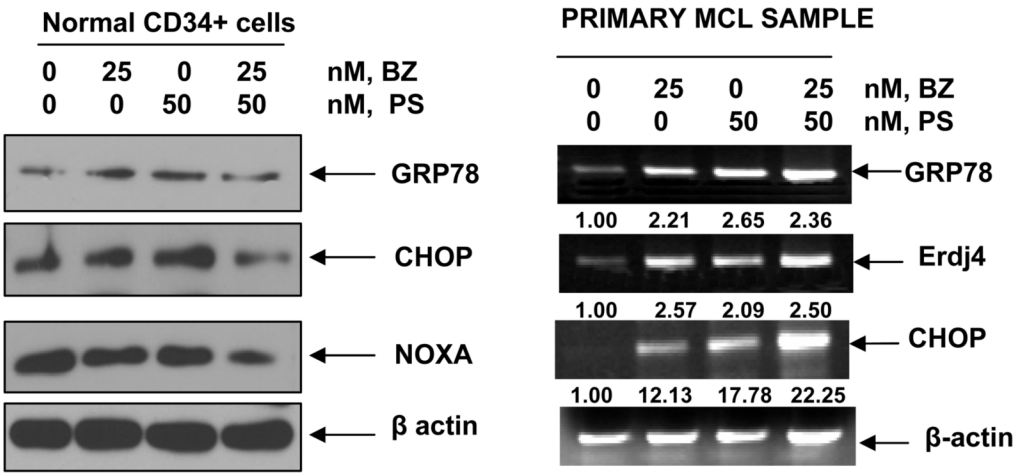

Figure 5. Effects of treatment with PS and/or BZ on primary MCL cells

Normal CD34+ cells were treated with indicated doses of PS and BZ for 24 hours and the expression of GRP78, CHOP and NOXA was assessed by western blot analyses. The expression of β-actin served as the loading control. Alternatively, primary MCL cells were treated with the indicated doses of PS and/or BZ for 24 hours and the expression of GRP78, Erdj4, CHOP and β-actin was assessed by RT-PCR analysis. Data presented here are representative of two independent experiments.

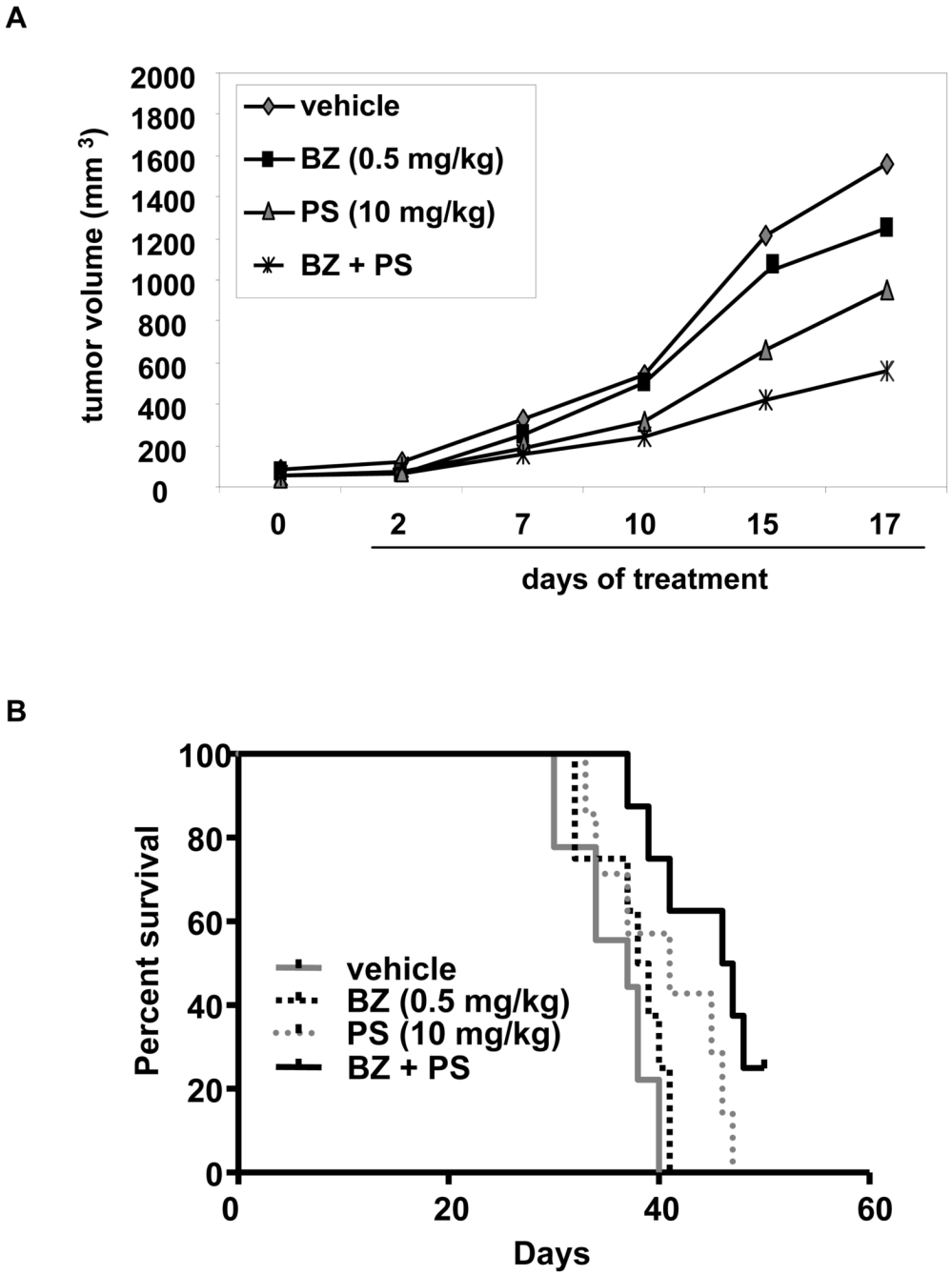

Figure 6. Co-treatment with BZ and PS inhibits in vivo tumor growth in Z138C xenografts

A, Regression of tumor volume (n=8) following treatment with PS, BZ and a combination of BZ and PS is depicted. **B,** Kaplan-Meier survival plot for a Z138C xenograft model of MCL: NOD-SCID mice (n=8/group) were injected with Z138C cells subcutaneously and treatment with BZ, PS and the combination was commenced when the average tumor volume reached 50 mm^3.

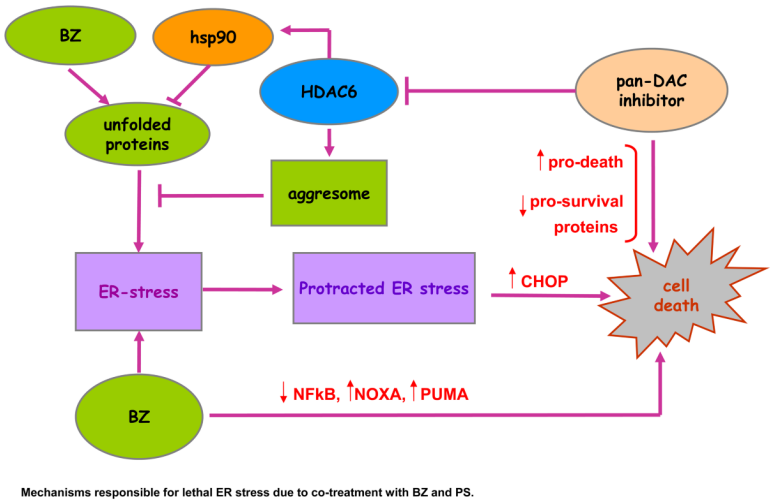

Figure 7. Mechanisms responsible for lethal ER stress due to co-treatment with BZ and PS

By inhibiting HDAC6 which shuttles misfolded, polyubiquitylated proteins into the protective organelle aggresome, co-treatment with BZ and PS increases the unfolded protein response and ER-stress. Protracted, unresolved ER stress leads to increased PS and BZ-induced cell-death.

Table 1

Panobinostat and/or BZ induces cell death of primary MCL cells

	% cell death of primary MCL samples			
sample	**control**	**25 nM, BZ**	**50 nM, PS**	**BZ + PS**
Normal CD34+	2.8 ± 0.2	9.3 ± 3.8	30.1 ± 2.0	33.5 ± 3.0
MCL#1	2.7 ± 0.2	5.4 ± 0.3	10.1 ± 1.6	25.6 ± 1.7 *
MCL#2	4.9 ± 2.0	27.7 ± 4.1	41.5 ± 1.2	51.5 ± 1.4 *
MCL#3	9.4 ± 0.5	23.8 ± 1.0	25.1 ± 1.7	64.9 ± 2.5**

NOTE: Primary MCL cells from three patients and normal CD34+ cells were treated in triplicate for 48 hrs with the indicated doses of PS and BZ. Following this, the average viability of cells was assessed using trypan blue dye exclusion and a hemocytometer

* $p \leq 0.05$,

** $p \leq 0.005$.

Values represent the percentage of dead cells ± standard deviation from each condition as compared with untreated cells.